Astron. Astrophys. 284, 424–436 (1994)

ASTRONOMY
AND
ASTROPHYSICS

# A Study of the color-magnitude diagrams and luminosity functions of the two LMC clusters NGC 2134 and NGC 2249 with the new radiative opacities*

**A. Vallenari[1], A. Aparicio[2], F. Fagotto[1], and C. Chiosi[1]**

[1] Dipartimento di Astronomia dell'Università di Padova, Vicolo dell'Osservatorio 5, I-35122, Padova, Italy
[2] Instituto de Astrofísica de Canarias , E-38200, La Laguna, Tenerife, Canary Islands, Spain

Received 23 August 1993 / Accepted 11 October 1993

**Abstract.** We present Johnson CCD photometry in the $B$ and $V$ passbands for the stellar content of two intermediate age star clusters of the Large Magellanic Cloud, NGC 2134 and NGC 2249. In total 1613 stars are measured in NGC 2134 and 850 in NGC 2249. With the aid of two grids of stellar models calculated with convective overshoot (both from the core and the envelope) and different radiative opacities, we examine the color-magnitude diagrams (CMDs) and luminosity functions (LFs) of the clusters and estimate reddening, metallicity, and age. The opacities in usage are either the classical ones by Huebner et al. (1977)(thereinafter LAOL) or those by Iglesias et al. (1992) (thereinafter OPAL). Adopting the distance modulus of $(m-M)_o$ = 18.5mag, we find that stellar models with metallicity Z=0.008 are best suited to match the main features of the observed CMDs. Accordingly, we get $E_{(B-V)}$ = 0.22 and the age of $1.9 \times 10^8$ yr for NGC 2134, and $E_{(B-V)}$ = 0.25 and the age of $5.5 \times 10^8$ yr for NGC 2249. Similar analysis is made using both the opacity source (OPAL or LAOL) bringing into evidence the major differences. Finally, for the sake of comparison we also examine the CMDs and LFs by means of models with identical opacities but the classical scheme of mixing. The LFs indicate that classical models with OPAL require unusually steep slopes of the initial mass function (IMF), $x$ = 3.35 or greater, whereas models with overshoot and OPAL are consistent with the classical slope, $x$ = 2.35.

**Key words:** convection – stars: evolution – globular clusters: NGC 2134, NGC 2249 (LMC) – galaxies: Magellanic Clouds – galaxies: star clusters

## 1. Introduction

Accurate stellar models are basic to many astrophysical problems, e.g. studies of star clusters, stellar pulsations, stellar nucleosynthesis, photometric and chemical evolution of galaxies, star formation process, etc.

Although current stellar models are quite accurate, still several causes of uncertainties are present. Among others, we recall the radiative opacities which have been greatly improved over the past few years with the advent of the new opacities by Rogers & Iglesias (1992) and Iglesias et al. (1992).

The main difference in OPAL with respect to the old ones by Huebner et al. (1977), is the presence of a bump-like enhancement at temperatures of a few hundred thousand degrees. The peak of the bump critically depends on the chemical composition, being higher at higher metal content. It is also related to whether or not the spin-orbit interactions are included, and to the mixture of the fractional abundances of metals adopted in the opacity calculations.

Somewhat older calculations of OPAL (Rogers & Iglesias 1992) neglected the spin-orbit interaction in the treatment of the Fe atomic data and adopted the solar abundance of [Fe/H] by Anders & Grevesse (1989). On the contrary, more recent versions of the same opacities (Iglesias et al. 1992) include the spin-orbit interactions and adopt new measurements for the solar photospheric abundance of [Fe/H] by Grevesse (1991) and Hannaford et al. (1992).

The inclusion of the spin-orbit interaction results in an enhancement of the bump of 50 % with the Anders & Grevesse (1989) mixture and of 25 % with the Grevesse (1991) composition.

These changes are far from being negligible, because the opacity affects considerably magnitudes, colors, and lifetimes of the evolutionary phases, and should be checkable in the observational data of star clusters.

Recently, Meynet et al. (1993) estimated the age of some Galactic open clusters on the basis of stellar models including

*Send offprint requests to*: A. Vallenari

* Based on observations obtained at the European Southern Observatory, La Silla, Chile

the new OPAL. These models however do not extend beyond the RGB tip, so that the comparison with the overall properties of the CMD is not possible. No analysis has been made of the luminosity functions.

The aim of this paper is first to acquire CCD photometric data of two star clusters of the Large Magellanic Cloud (LMC), namely NGC 2134 and NGC 2249, in the Johnson BV passbands, and second to analyze the CMDs and LFs by means of stellar models calculated with OPAL and LAOL in order to check for the differences originating from the two sources of opacity in usage.

The stellar models with OPAL are from the library of evolutionary tracks by Bressan et al. (1993) and Fagotto et al. (1993a,b), whereas those with LAOL are from Alongi et al. (1993). All the models are based on the overshoot scheme for the treatment of core and envelope convection (see below for more details). However, whenever necessary the analysis will be also extended to considering models with the same opacities but with the classical scheme of mixing calculated by the same authors.

NGC 2134 ($\alpha = 5^h52^m38^s$, $\delta = -71°07'.1$ at 1950) is classified as type IV in the system of Searle et al. (1980). Following van den Bergh (1981), its apparent integrated magnitude is $V = 11.05$ mag and its color indices are $(B-V) = 0.25$ and $(U-B) = 0.02$. Elson (1986) gives the color excess $E(B-V) = 0.13$ in agreement with the value of $E(B-V) = 0.14$ determined by Cassatella et al. (1987) and the value of $E(B-V) = 0.20$ determined by Hodge & Schommer (1984). Ages have also been estimated by these authors. They obtain $(1.1 \pm 0.2) \times 10^8$ yr (Hodge & Schommer 1984), and $1 \times 10^8$ yr (Elson 1986). Moreover, Elson (1986) estimates a metallicity of $[Fe/H] = -0.5$. Carbon stars have been found by Westerlund et al. (1991).

Little attention has been devoted to NGC 2249 ($\alpha = 6^h26^m06^s$, $\delta = -68°53'.0$ at 1950) before this study. Its integrated magnitude and color indices, according to van den Bergh (1981), are $V = 12.23$ mag, $(B-V) = 0.43$ and $(U-B) = 0.20$. Elson (1986) estimates an age of $5 \times 10^8$ yr. Previous CMD is by Jones (1987).

Section 2 reports the observations and data reduction, and presents the raw CMDs of the clusters and companion fields. Section 3 deals with the correction for incompleteness and contamination by foreground stars, and describes the reference CMDs and the LFs. Section 4 analyses the CMDs and presents the ages obtained from the comparison with the theoretical models including convective overshoot and both OPAL and LAOL opacities. Section 5 discusses the LFs first for the same models used to analyze the CMDs and then also for models with the same opacities but the classical scheme of mixing. Finally, Section 6 summarizes the results and draws some conclusions.

## 2. Observations, data reduction, and color-magnitude diagram

NGC 2134 and NGC 2249 were observed in December 1987, using the 512 × 320 pixels (pxl) thin ESO RCA CCD #5 at the Cassegrain focus of the 2.2 m telescope at La Silla (Chile). The pixel size was 30$\mu$m, providing a scale of 0.363"/pxl.

In addition to this, two fields near the clusters were also observed to correct the cluster CMDs for the contamination by foreground stars. The observations were taken in September 1988, using the 1.5m Danish telescope at La Silla (Chile) and the $1024 \times 640$ pixels thin ESO RCA CCD #8, rebinned to $2 \times 2$. Thus, the effective pixel was also 30$\mu$m, providing a scale of 0.47"/pxl at the Cassegrain focus of the telescope.

A number of standard stars from the list of Landolt (1983) were also observed, to derive the transformation equations from the instrumental to the Johnson systems.

Table 1 shows the journal of observations. The last column gives the stellar full width at half maximum measured in each frame.

The frames have been processed with MIDAS, DAOPHOT and ALLSTAR (see Stetson 1987) to obtain the photometry of the stars both in the clusters and companion fields.

The calibration of the magnitudes of the stars in NGC 2249 is made by means of the synthetic aperture photometry together with the average extinction at La Silla. The instrumental to Johnson transformation equations for an integration time of 5 minutes are:

$$V - v = -0.016(B-V) + 3.54 \quad (1)$$

$$(B-V) = 1.11(b-v) - 0.67 \quad (2)$$

where capital letters are Johnson magnitudes and small letters are instrumental magnitudes.

In the case of NGC 2134 the photometry is calibrated with the aid of the calibration obtained by Hodge & Schommer (1984). The transformation equations for an integration time of 5 minutes are:

$$V - v = -0.016(B-V) + 3.24 \quad (3)$$

$$(B-V) = 1.17(b-v) - 0.784 \quad (4)$$

In both cases, the $\sigma$ of the zero points are 0.04 for the transformation of $V$, and 0.05 for that of $(B-V)$.

Finally, the transformation for the field stars (integration time of 8 minutes) are:

$$V - v = -0.017(B-V) + 2.748 \quad (5)$$

$$(B-V) = 1.09(b-v) - 2.390 \quad (6)$$

The $\sigma$ values of the zero points are 0.02 for the transformation of $V$, and 0.03 for that of $(B-V)$.

In total, we have measured the $B$ and $V$ magnitudes of 1613 stars in NGC 2134, and 850 in NGC 2249. For the sake of conciseness, the magnitudes and colors of all measured stars in the cluster and field frames are not given here, but are made available from the authors on request.

For purposes of illustration we show in Figs. 1a and 1b the position of the stars measured in the frame of NGC 2134 and

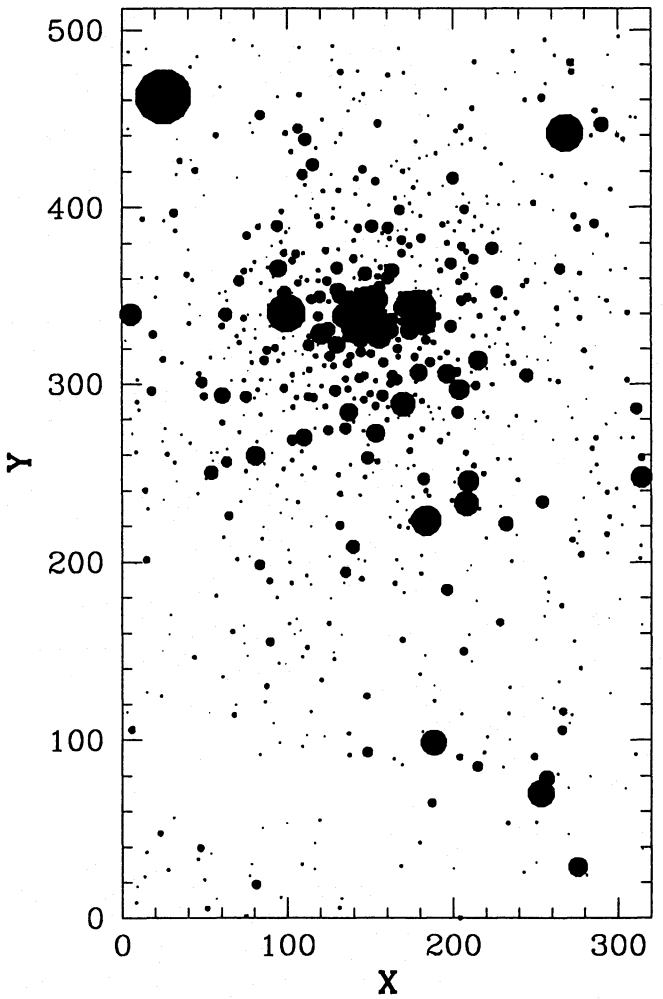


**Fig. 1a.** Identification chart of the stars detected in the frame of NGC 2134. The size of the circles is proportional to the brightness in $V$. Coordinates are in CCD pixels. North is at the top and East is at the left

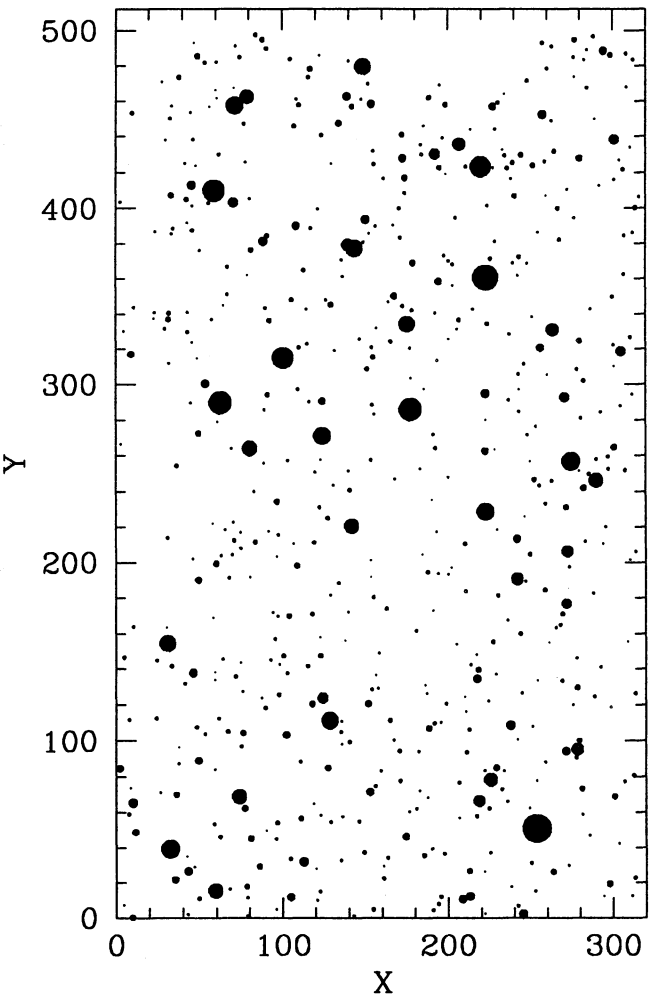


**Fig. 1b.** Identification chart of the stars detected in the companion field of NGC 2134. The size of the circles is proportional to the brightness in $V$. Coordinates are in CCD pixels. North is at the top and East is at the left

companion field, respectively, while in Figs. 2a and 2b we show the same but for NGC 2249. The coordinates are CCD pixels and the size of the circles are proportional to the brightness in $V$ of each star.

The determination of the photometric errors in crowded frames has already been discussed by various authors. In the following, we adopt the artificial star method (see Vallenari et al. 1992 for a detailed description). In the case of NGC 2134, the errors (standard deviations) are 0.03, 0.05, 0.07 at $V = 18, 19, 20$ mag respectively. The errors are comparable for NGC 2249 and slightly lower for the companion fields.

The raw CMDs of the clusters and companion fields are shown in Figs 3a and 3b for NGC 2134 and Figs.4a and 4b for NGC 2249. It is worth recalling that the total number of stars in the cluster CMD is not comparable to that in the field CMD because they have a different coverage of the sky due to the different telescopes in use. Re-normalization of the star counts is required.

## 3. Correction for incompleteness and field stars

Correction for incompleteness and foreground stars is particularly important to derive the LF of main sequence stars, which constitutes a key constraint in the comparison of the observational data with the theoretical models, synthetic CMDs and LFs.

The correction for incompleteness stands on the usual technique of the artificial star experiments, following the procedure outlined by Stetson & Harris (1988). This is applied to the frames both of the cluster and companion field.

For each frame ($B$ and $V$), we have performed 30 experiments adding a small percentage of stars (less than 10% of the total number). The artificial stars are injected in the same positions in the $B$ and $V$ frames, adopting a color mimicking the instrumental color index of the corresponding main sequences. This enables us to check that the completeness factors for the $B$ and $V$ pass-bands are not independent and that to a good approximation those of the $B$ frames are to be preferred. In-

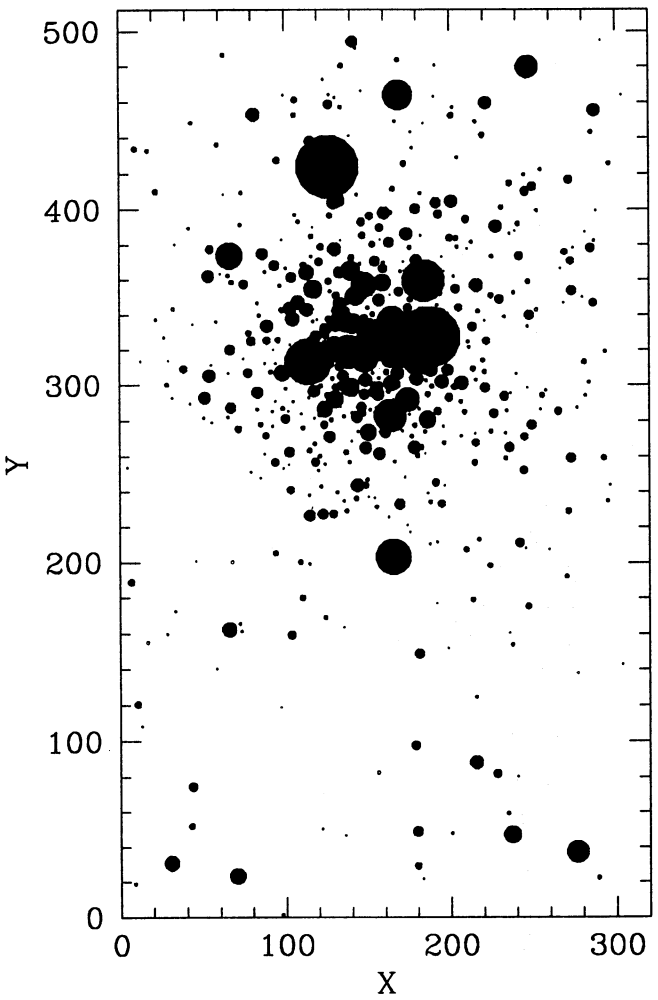


**Fig. 2a.** Identification chart of the stars detected in the frame of NGC 2249. The size of the circles is proportional to the brightness in $V$. Coordinates are in CCD pixels. North is at the top and East is at the left

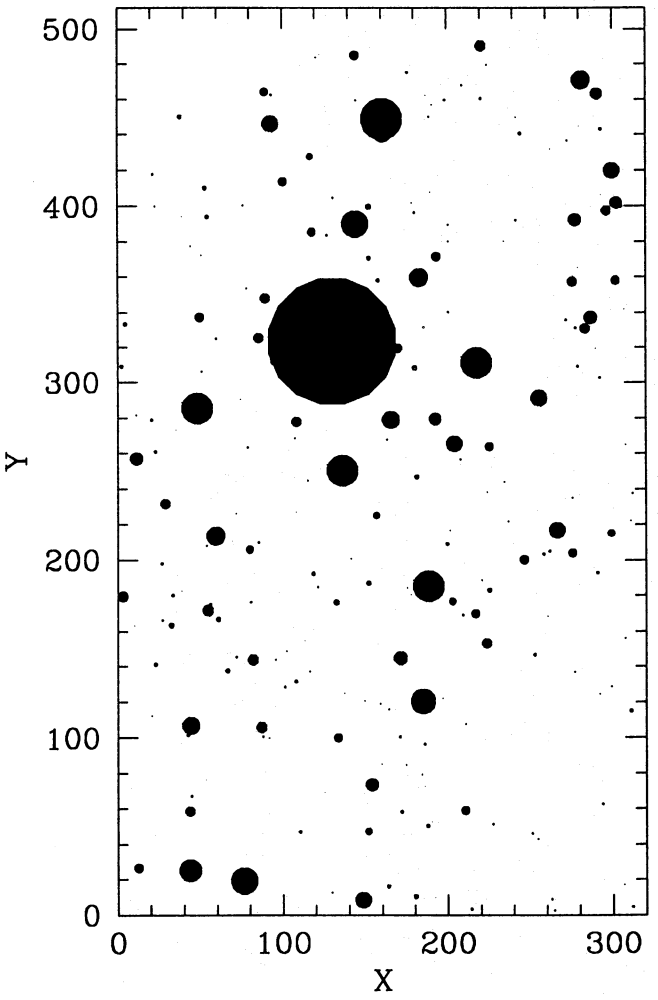


**Fig. 2b.** Identification chart of the stars detected in the companion field of NGC 2249. The size of the circles is proportional to the brightness in $V$. Coordinates are in CCD pixels. North is at the top and East is at the left

deed, when an artificial star is not recovered in the $V$ frame, this usually happens also in the corresponding $B$ frame, but the contrary is not true.

To select the regions of the cluster frames where the incompleteness is not critical, we first derive the centers of the clusters, calculating the unweighted means of the X and Y coordinates of the stars from a provisional eye-estimated center until the convergence is achieved. We derive $X_c$=148.43 pxl and $Y_c$ =334.45 pxl for NGC 2134 and $X_c$ =156.20 pxl , $Y_c$ =326.10 pxl for NGC 2249. We find that for both clusters, the region within a circle of radius 50 pixels centered on ($X_c$,$Y_c$) is severely affected by incompleteness as there the mean crowding is higher than 50% and the incompleteness correction is not reliable. Therefore this region is excluded in the derivation of the CMD and LF.

For both clusters, the incompleteness factors $\Lambda$ (defined as the number of artificial stars recovered divided by the number of artificial stars added to the $B$ frames for each magnitude interval) are listed in Table 2 for radii larger than 50 pxl.

In order to apply the correction for incompleteness and remove foreground stars from the CMD and LF of the clusters, we divide the CMD of the cluster and companion field in subregions. We first correct each region for incompleteness and second, we subtract from each region of the cluster CMD the number of stars found in the corresponding region of the field CMD. The star counts are suitably scaled to account for the different sky coverage of the cluster and field frames.

The above procedure is strictly followed to derive the LF of the MS stars. However to discuss the CMD morphology of each cluster we prefer to look at the CMD to which only the correction for foreground stars is applied. These CMDs are shown in Fig. 5a for NGC 2134 and Fig. 5b for NGC 2249.

The salient features of these CMDs can be summarized as follows. In the CMD of NGC 2134, the clump of the core He-burning stars is located at approximately $0.80 \leq (B-V) \leq$

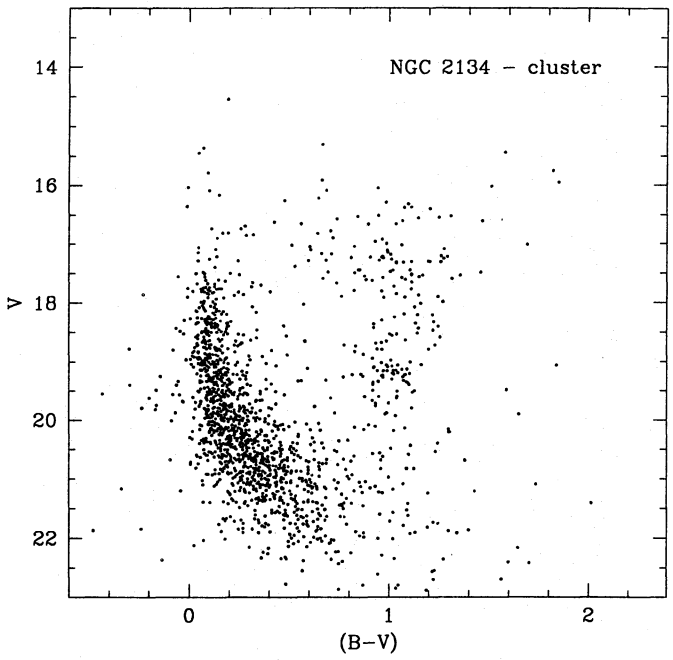


**Fig. 3a.** The raw CMD of NGC 2134. Apparent magnitudes and colors are shown

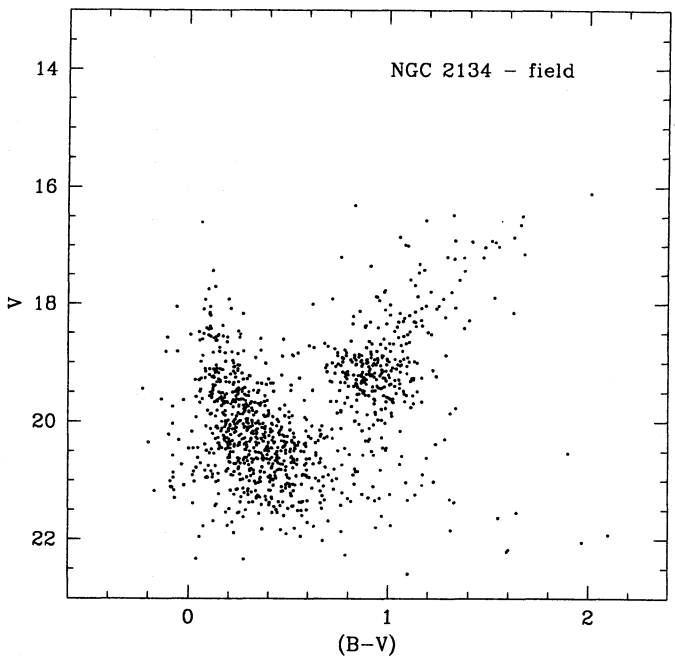


**Fig. 3b.** The raw CMD of the companion field of NGC 2134. Apparent magnitudes and colors are shown

**Table 1.** Journal of Observations

| Object | Date | Filter | Exp. time(s) | FWHM (") |
|---|---|---|---|---|
| NGC 2134 | Dec.18.1987 | *B* | 360 | 1.0 |
| NGC 2134 | Dec.18.1987 | *V* | 360 | 1.0 |
| NGC 2134/field | Sep.20.1988 | *B* | 540 | 1.3 |
| NGC 2134/field | Sep.20.1988 | *V* | 420 | 1.3 |
| NGC 2249 | Dec.18.1987 | *B* | 300 | 1.0 |
| NGC 2249 | Dec.18.1987 | *V* | 300 | 1.0 |
| NGC 2249/field | Sep.18.1988 | *B* | 540 | 1.3 |
| NGC 2249/field | Sep.18.1988 | *V* | 420 | 1.3 |

1.13, $16.5 \leq V \leq 17.5$ mag (Fig. 5a) and it is likely contaminated by foreground stars. The eye-drawn line in Fig. 5a provisionally separates main-sequence (MS) stars from red evolved stars. Most likely, the MS turnoff is at $V \simeq 17.1$ mag, but a few brighter stars are seen up to $V \simeq 14.5$ mag (the nature of these stars will be examined in more detail below). A great number of evolved stars (RG) populates the diagram up to $V \simeq 15.5$ mag and $0.4 \leq (B-V) \leq 1.9$.

In the CMD of NGC 2249, the MS turnoff is as bright as $V \simeq 18.5$ mag. The clump of the red evolved stars is centered at $V \simeq 19.0$ mag, $(B-V) \simeq 0.9$. Also in this case, the line drawn in Fig. 5b separates the approximate location of MS stars from the evolved ones. It is also evident from the scarcely populated CMD of the companion field that the contamination by foreground stars is less of a problem than for NGC 2134.

Concerning the CMDs of the companion fields already presented in Figs. 3b and 4b, the following remarks can be made. In the case of NGC 2134, the MS band extends up to $V \simeq 17.4$ mag, there is a well-populated red clump, and the red giant and asymptotic giant branches (RGB and AGB, respectively) reach $V \simeq 16.5$ mag, $(B-V) \simeq 1.68$. In the case of NGC 2249, the MS likely terminates at $V \simeq 18.7$ mag. However the clumps of the red evolved stars for the cluster and the field fall in the same region of the CMD, thus making the correction for the contamination by field stars more uncertain.

Finally, the observational LFs for the main sequence stars of the clusters after correction for completeness and foreground star contamination are shown in Fig. 6.

Before concluding this section, we address the question whether the MS termination magnitude can be biased by the presence of a certain fraction of *binary* stars, either caused by the alignment of two stars along the line of sight or physical.

In our frames, two stars with separation smaller than about 0.4 FWHM cannot be resolved by our measuring package. In the case of NGC 2134 this corresponds to about 1.6 pxl. In the area of 270×300 pxl, where the density of stars is higher, 870 stars are detected. If these objects are distributed at random, the probability that a star has a companion within 1.6 pxl is about 0.13. To significantly increase the magnitude of the resulting object, the secondary star must be at the most one magnitude fainter than the primary. So, the final probability might be lower by a factor of 4, since the stars are distributed over a range of four magnitudes. This calculation does not take into account the presence of a density gradient in the field that can partially compensate for this last condition. We can reasonably say that the final probability of finding optical binaries amounts to 0.13-0.03. The condition that some binaries are present would shift the turnoff 0.7 mag fainter than the observed at V=17.96 mag. In the raw CMD of Fig. 3a, we find 24 stars brighter than V=17.96 mag and 84 stars in the range V=17.96 to 18.66 mag. If all

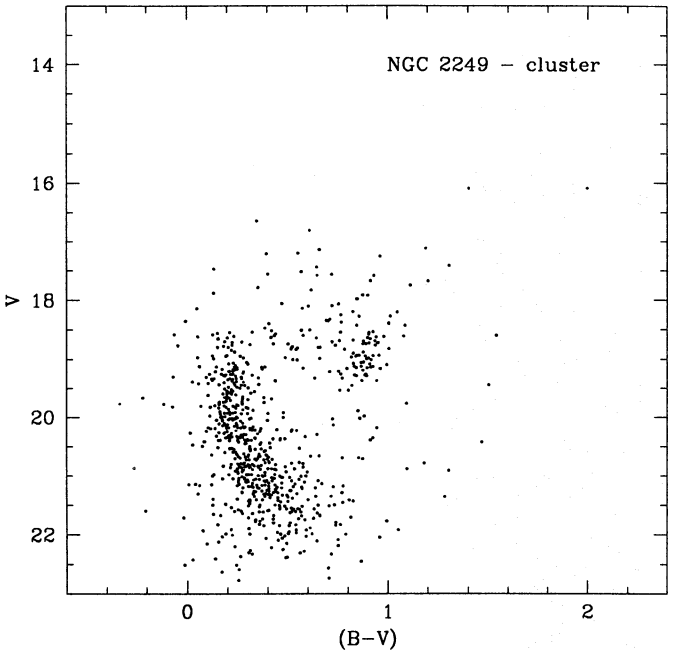


**Fig. 4a.** The raw CMD of NGC 2249. Apparent magnitudes and colors are shown

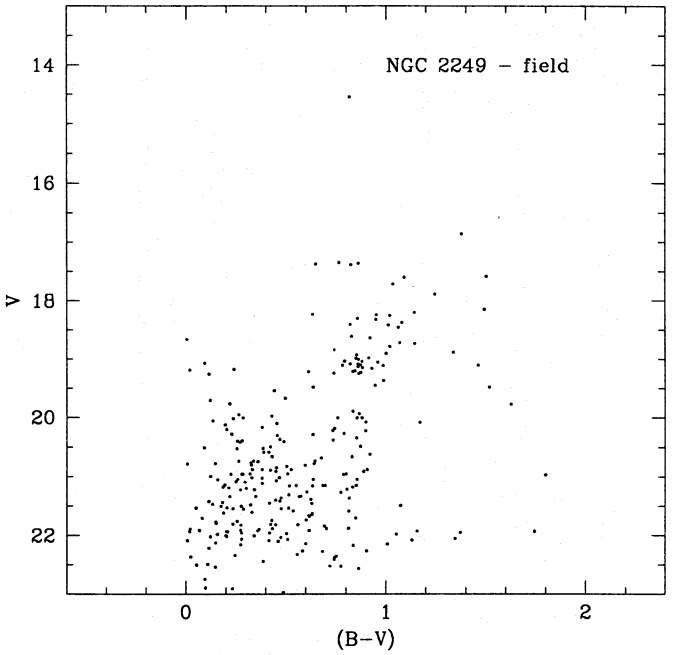


**Fig. 4b.** The raw CMD of the companion field of NGC 2249. Apparent magnitudes and colors are shown

the brightest stars are binaries, we find that the probability for binarity is about 0.22, significantly higher than the expected percentage of optical binaries. Although these calculations are too approximate to derive the percentage of true binaries in NGC 2134, there might be the indication that some of these stars may be physically connected. In the analysis below we will always include a certain percentage of binary stars, because at least the optical ones are present.

In the case of NGC 2249, we calculate the probability for optical binaries in an area of 270× 300 pxl surrounding the center of the cluster. We get a probability in the range 0.08 to 0.023. Comparing the number of MS stars in the magnitude bins 0.7 mag brighter and fainter than the termination magnitude of the MS, we get a percentage of binaries of 0.14. As in the case of NGC 2134, we can conclude that binaries, either optical or physical, are likely to be present in the cluster.

**Table 2.** Completeness factors in B

| | NGC 2134 field | NGC 2134 | NGC 2249 field | NGC 2249 |
|---|---|---|---|---|
| $B$ | $\Lambda$ | $\Lambda$ | $\Lambda$ | $\Lambda$ |
| 17.75 | 1.00 | 1.00 | 1.00 | 1.00 |
| 18.25 | 0.98 | 1.00 | 1.00 | 1.00 |
| 18.75 | 0.97 | 1.00 | 0.98 | 1.00 |
| 19.25 | 0.95 | 1.00 | 0.97 | 1.00 |
| 19.75 | 0.87 | 0.85 | 0.95 | 1.00 |
| 20.25 | 0.83 | 0.91 | 0.91 | 1.00 |
| 20.75 | 0.77 | 0.85 | 0.87 | 0.92 |
| 21.25 | 0.60 | 0.65 | 0.83 | 0.85 |
| 21.75 | 0.45 | 0.35 | 0.75 | 0.77 |
| 22.25 | 0.25 | | 0.60 | 0.45 |

## 4. Analysis of the CMDs and LFs

The analysis of the CMDs and LFs stands on the method of synthetic CMDs and LFs described by Chiosi et al. (1989) and Vallenari et al. (1992) to whom the reader should refer for details. As already recalled the stellar models in use are from the libraries of stellar tracks calculated by Alongi et al. (1993), Bressan et al. (1993), and Fagotto et al. (1993a,b). The libraries include models in the mass range from 0.5 $M_\odot$ to 120 $M_\odot$, that are evolved from ZAMS to the start of the thermal pulsing regime of the AGB phase or carbon ignition as appropriate to the initial stellar mass. Models are available for two different schemes of mixing, i.e either classical mixing (Schwarzschild criterion for the border of the H-burning convective core and semiconvection during the central He-burning), or overshoot (mixing of the material beyond the formal convective core), and two sources of radiative opacities, namely either LAOL or OPAL.

The efficiency of convective overshoot is formulated according to Bressan et al. (1981) and Alongi et al. (1993) and it is parameterized by the ratio $\lambda$ between the distance travelled by convective elements and the local pressure scale height. According to Alongi et al. (1993) the parameter $\lambda$ is $\lambda_c = 0.5$ for the core convection and $\lambda_e = 0.7$ for the envelope convection. All details concerning the treatment of convection in the classical scheme can be found in Alongi et al. (1993) to whom we refer.

In the discussion below, first we will adopt models with overshoot to assign the age and to point out the major differences caused by the opacity (OPAL versus LAOL), second limited to the case of OPAL we will examine the effect caused by different types of mixing, namely classical or overshoot, on the luminos-

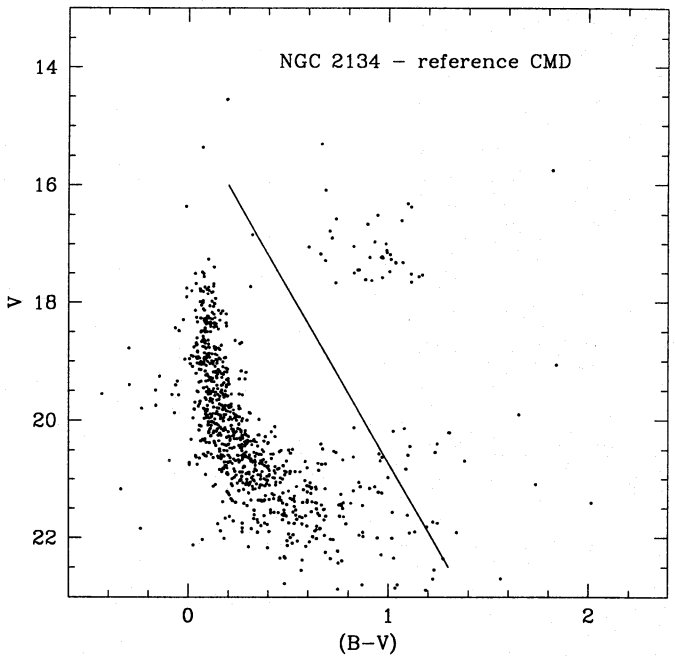


**Fig. 5a.** The reference CMD for the cluster NGC 2134

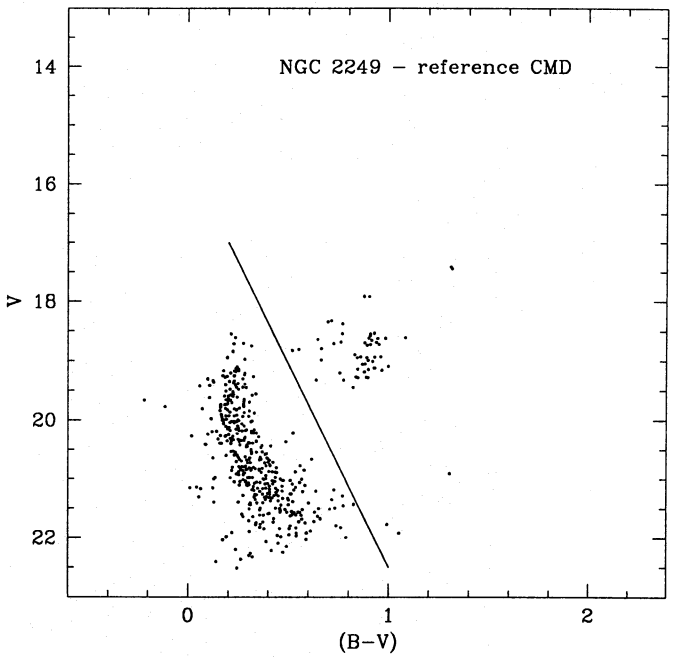


**Fig. 5b.** The reference CMD for the cluster NGC 2249

ity function. The reason for this is that the LF is more sensitive to the mixing in use than to the morphology of the CMD.

Finally, in this study we assume that the distance modulus of both clusters is the mean modulus of the LMC, and adopt $(m - M)_0$ = 18.5mag, in agreement with the value suggested by various authors (Westerlund 1991; Panagia et al. 1991; Hanuschik & Schmidt-Kaler 1991).

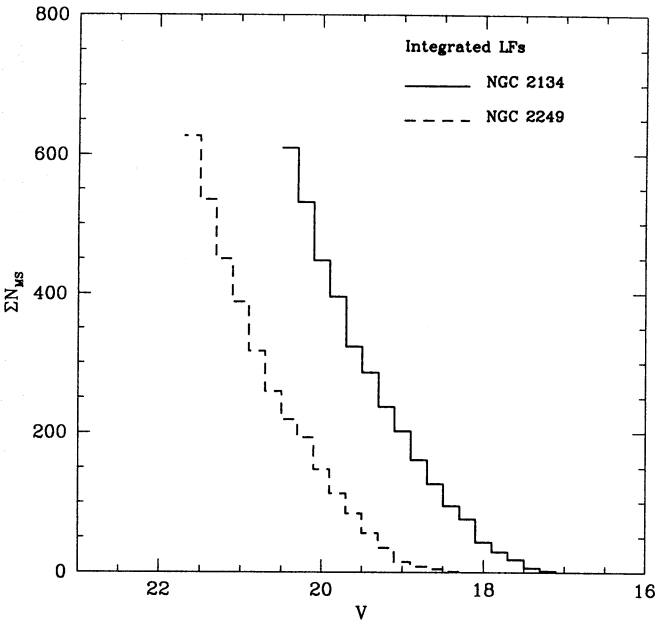


**Fig. 6.** The integrated LF of the MS stars of NGC 2134 and NGC 2249

### *4.1. The CM diagram of NGC 2134*

A preliminary comparison of the observational CMD with the synthetic ones indicates that metallicity Z=0.008 and reddening $E(B-V) = 0.22$ are a reasonable choice. A lower reddening is compatible with a much lower metallicity, but in such a case, the evolved stars would be too red with respect to model predictions.

With the assumed distance modulus, reddening and metallicity, the faintest evolved stars are at $M_{V_0} = -1.5$ mag and the top of the MS is at $M_{V_0} = -1.9$ mag, which considering the probable effect of binary stars becomes $M_{V_0} = -1.2$ mag. Independently of the opacity in use, this corresponds to an age of $1.9 \times 10^8$ yr.

Figure 7 shows two isochrones for the age of $1.9 \times 10^8$ calculated with OPAL and LAOL opacities as indicated. The turnoff mass is about 3.9 $M_\odot$. It is evident that the turnoff luminosity is not greatly affected by the opacity in usage. As a matter of fact, with OPAL the core H-burning models are slightly cooler and fainter than with LAOL, but the effect is small since the bump in OPAL is located too far out in the external envelope, and therefore it does not affect appreciably the internal structure and hence luminosity of the star (see Bressan et al. 1993 for a wide discussion).

The RGB and AGB phases of models with OPAL shift toward slightly hotter temperatures compared to models with LAOL because of the different value of the mixing length parameter of the outermost convection that is required to match the Sun at varying opacity input. With OPAL this parameter turns out to be slightly higher than with LAOL (see Alongi et al. 1993; Bressan et al. 1993 for details).

The largest difference is in the luminosity of the faintest stars of the red clump (core He-burners). Specifically, with LAOL the bottom of the clump is about 0.42 mag more luminous than

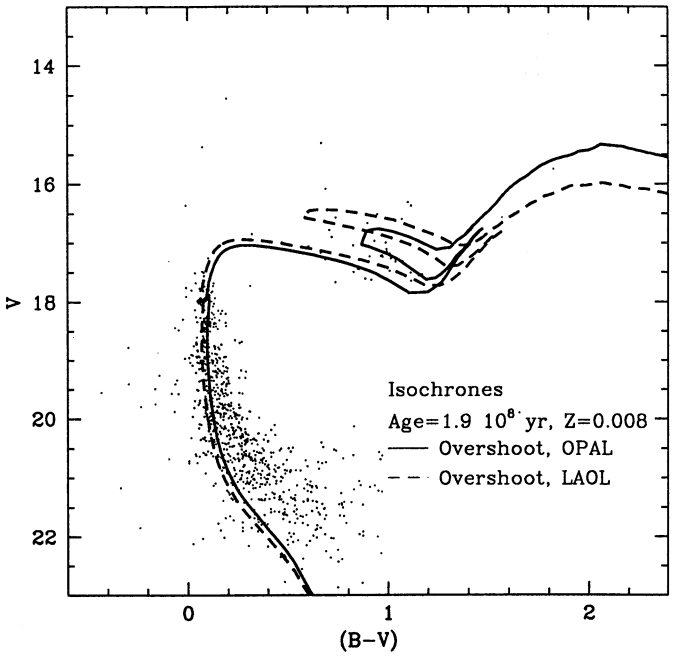


**Fig. 7.** The CMD of Fig. 5a superposed on the isochrones for the age of $1.9 \times 10^8$ yr calculated from stellar models with metallicity Z=0.008, convective overshoot, and two different sources of opacity using OPAL (full line) and LAOL (dashed line)

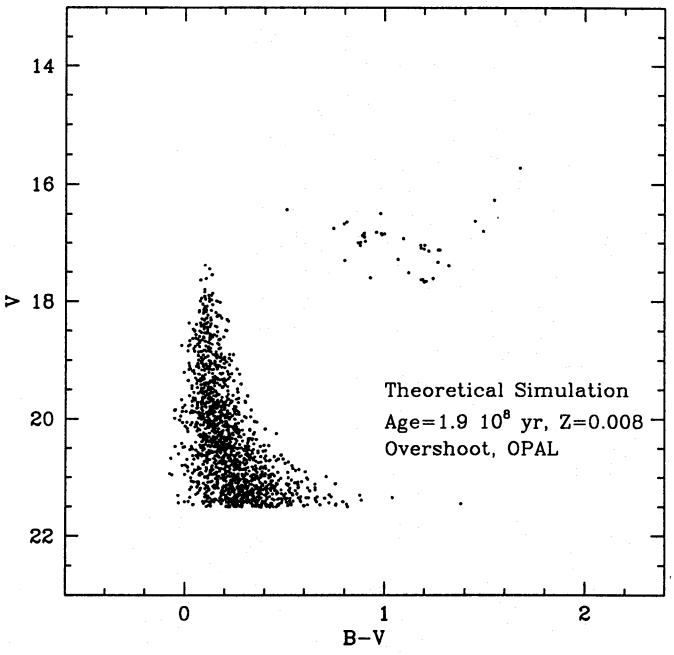


**Fig. 8a.** Synthetic CMD aimed to represent the CMD of NGC 2134. In these simulation models are used with metallicity Z=0.008, convective overshoot, and OPAL. The simulated CMD has the age of $1.9 \times 10^8$ yr, and the Salpeter IMF. Binary stars are included in the simulation, with the percentage of 20% and mass ratios in the range 0.8 to 1. Photometric errors are taken into account

the turnoff, whereas with OPAL this magnitude difference is reduced to about 0.2 mag.

Finally, OPAL produces clumps less extended in the blue of about 0.3 mag.

To disentangle which type of stellar models best matches the CMD of NGC 2134 is a cumbersome affair. Looking at the magnitude difference between the termination of the MS and the faintest evolved stars, it seems that models with OPAL are in closer agreement. This is shown by the synthetic CMD of Fig. 8a. This is obtained by adopting models with overshoot, OPAL, and age of $1.9 \times 10^8$ yr, and including a certain percentage of binary stars with suitable mass ratios. The percentage amounts to 20% and the mass ratios are in the range 0.8 to 1.0. Photometric errors, as determined from the artificial stars experiments, are taken into account in order to directly compare with the observed CMD. While the extension of the observed clump toward the blue is well reproduced, the red edge of this is bluer than predicted by the models. Figure 8b shows the same but for models with LAOL. Now the agreement with the observational CMD is poorer.

Finally, we notice the presence of too many red AGB stars in both simulations. Possible ways out of this discrepancy are either a different type of luminosity-core mass relation indicated by the models of Blöcker & Schönberner (1991) incorporating envelope burning or a different efficiency of mass loss along the AGB phase (see Chiosi et al. 1992 for detailed discussion of this topic).

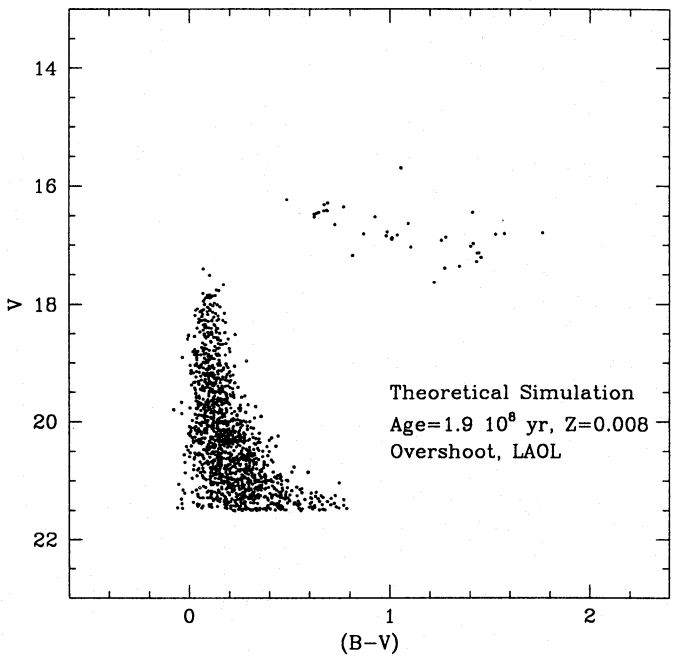


**Fig. 8b.** The same as in Fig. 8a, but for LAOL

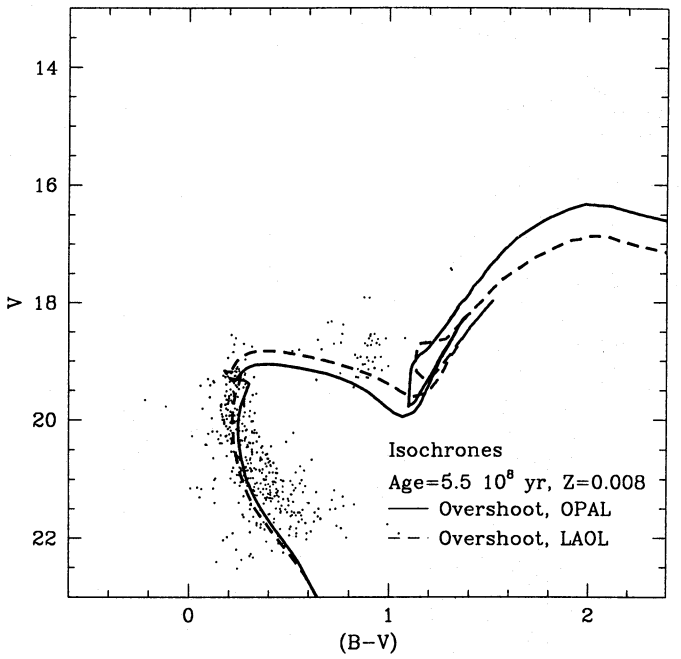


**Fig. 9.** CMD of Fig. 5b superposed on the isochrones for the age of $5.5 \times 10^8$ yr calculated from stellar models with metallicity Z=0.008, convective overshoot, and two different sources of opacity using OPAL (full line) and LAOL (dashed line)

### *4.2. The CM diagram of NGC 2249*

Reddening and metallicity suited to the CMD of NGC 2249 are $E(B-V) = 0.25$ and Z=0.008 and in turn the magnitude of the MS termination is $M_{V_0} = -0.8$ mag, which after correction for the probable presence of binary stars becomes $M_{V_0} = -0.2$ mag. This latter value and the use of stellar models with overshoot imply an age of $5.5 \times 10^8$ yr almost independently of the opacity.

Figure 9 compares two isochrones with the age of $5.5 \times 10^8$ yr, calculated using LAOL and OPAL, respectively. The turnoff mass is about 2.4 $M_\odot$. However, in this case the effect of the new opacities is slightly more relevant than in the previous one. Specifically, with OPAL the MS termination luminosity is fainter by about 0.15 mag and slightly redder than with LAOL, while the luminosity of the bottom of the clump of the core He-burning stars is about 0.4 mag fainter than with LAOL. It follows from this that with LAOL the turnoff and the bottom of the clump are about at the same luminosity, whereas with OPAL the clump is about 0.4 mag fainter than the MS termination.

Looking at the observational CMD, models with OPAL better fit the magnitude difference between the MS termination and bottom of the red clump. However, also in this case the theoretical colors of the stars in the clump are somewhat bluer than observed.

Finally, two synthetic CMDs for the age of $5.5 \times 10^8$ yr obtained with convective overshoot, a suitable fraction of binary stars and OPAL or LAOL are shown in Figs. 10a and 10b, respectively, for the sake of comparison with the observational CMD. The percentage of binary stars amounts to 20%, while

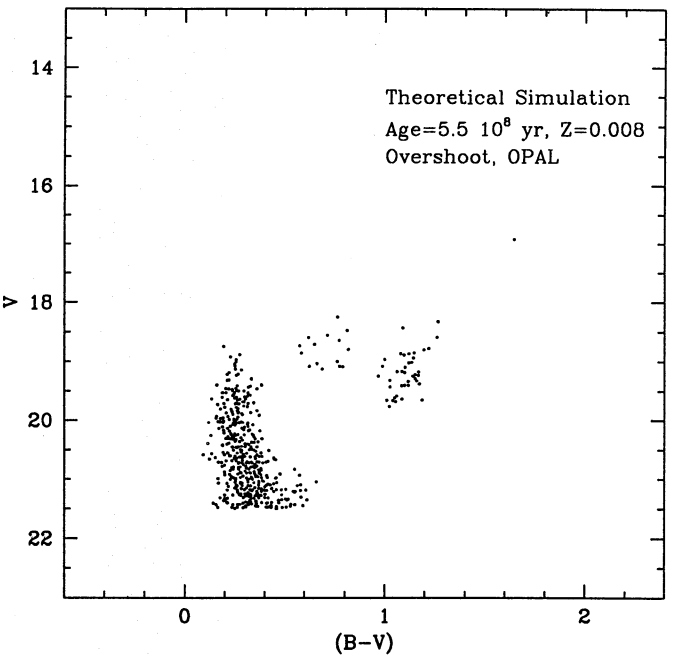


**Fig. 10a.** Synthetic CMD aimed to represent the CMD of NGC 2249. In these simulation models with metallicity Z=0.008, convective overshoot, and OPAL are used. The simulated CMD has the age of $5.5 \times 10^8$ yr, and the Salpeter IMF. Binary stars are included, with the percentage of 20% and mass ratios in the range 0.8 to 1. Photometric errors are taken into account

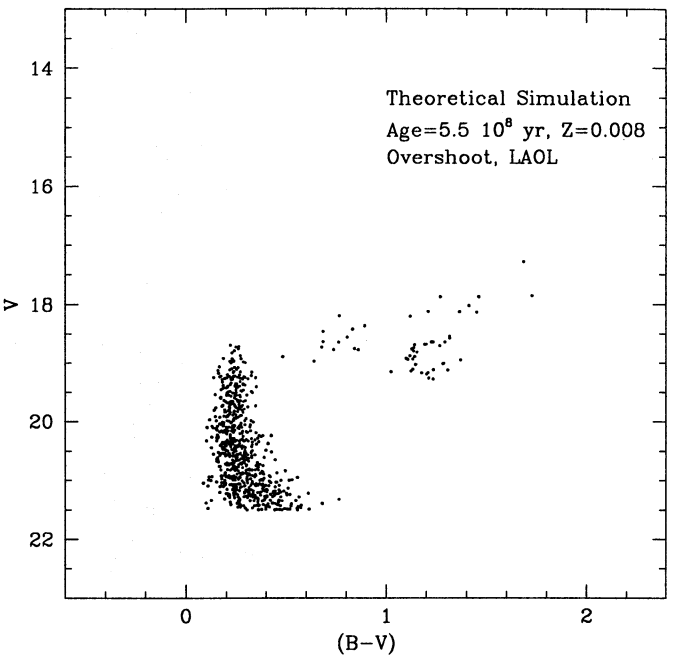


**Fig. 10b.** The same as in Fig. 10a, but using LAOL

their mass ratios are in the range 0.8 to 1. As in the case of NGC 2134, photometric errors are included.

## 5. Effects of opacities on the luminosity functions

The integrated luminosity function of the main sequence stars normalized to the number of red giants (NILF) is known to be related to the ratio of the core H- to He-burning lifetimes (Chiosi et al. 1989). The lifetimes of the stellar models in use are reported in Table 3 (models with overshoot) and 4 (models with classical scheme) for the case of OPAL and LAOL. These lifetimes are taken from Alongi et al. (1993), Bressan et al. (1993), and Fagotto et al. (1993a,b).

The data of Tables 3 and 4 clearly indicate that in addition to the type of mixing, the lifetimes and their ratios also depend very much on the opacity, the core He-burning lifetime ($\tau_{He}$) in particular. Specifically, in the range of intermediate mass stars, while the core H-burning lifetime is not too affected by using OPAL instead of LAOL, $\tau_{He}$ turns out to be even 60% larger than with LAOL in masses just higher than the minimum mass for quiet central He-burning ($M_{Hef}$).

The success of the NILF as a probe of the lifetime ratio is however hampered by the uncertainty in identifying among the evolved stars of a CMD the sample corresponding to cluster stars in core He-burning. Indeed the population of post MS stars (fewer in number) can be severely contaminated by field stars. Fortunately, in the CMDs of both NGC 2164 and NGC 2249 the contamination by field stars is less of a problem. As a matter of fact, in the case of NGC 2134 the cluster red giants are significantly brighter than the field giants, in the case of NGC 2249, owing to the scarce population in the field, the contamination by this type of stars should be small. However, we cannot rule out that, even after careful subtraction of field stars, some contamination is still present.

We first discuss the case of models with overshoot and show how the NILF varies passing from LAOL to OPAL. On the observational side, the NILF is obtained from the ILF after correction for completeness and foreground contamination (Fig. 6) divided by the number of evolved stars identified in the CMD of the clusters. The number of evolved stars are $N_{ev}$=40 for NGC 2134 and $N_{ev}$=57 for NGC 2249. On the theoretical side the NILFs are derived from the simulated CMD assuming the same ages and fractions of binary stars adopted in the interpretation of the CMDs. The slope $x$ of the IMF is let vary. The observational NILFs are shown in Figs.11a and 11b together with their theoretical counterparts for NGC 2134 and NGC 2249, respectively.

In the case of NGC 2134, NILFS from models with OPAL and LAOL are both compatible with $x$ = 2.35, i.e. the classical value of Salpeter. However in the case of OPAL, the slope $x$ = 3.35 cannot be excluded. In the case of NGC 2249, the observational NILF is compatible either with OPAL and $x$ = 3.35 or LAOL with $x$ = 2.35.

It has been repeatedly argued (Brocato et al. 1990; Stothers & Chin 1991; Castellani et al. 1992) that the changes in stellar lifetimes produced by OPAL would make unnecessary to in-

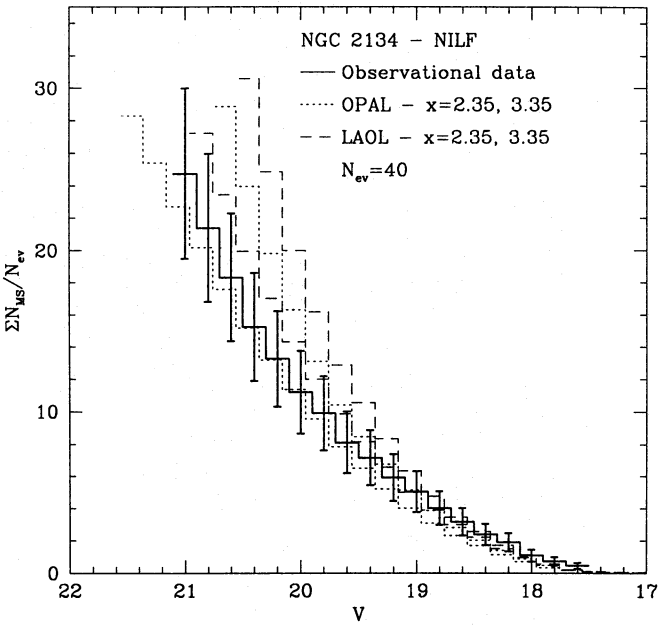


**Fig. 11a.** Integrated luminosity function (NILF) of the MS stars normalized to the number of evolved stars in NGC 2134 (solid line) compared with theoretical NILFs for the age of 1.9 $\times 10^8$ yr. The theoretical NILFs are calculated with OPAL (dashed lines) and LAOL (dotted lines), a suitable fraction of binary stars, and different values of the IMF slope $x$ as indicated. For each group, the slope gets steeper going upward. Absolute magnitudes are converted to apparent ones assuming $(m - M)_o$ = 18.5 and $E_{B-V}$ = 0.22

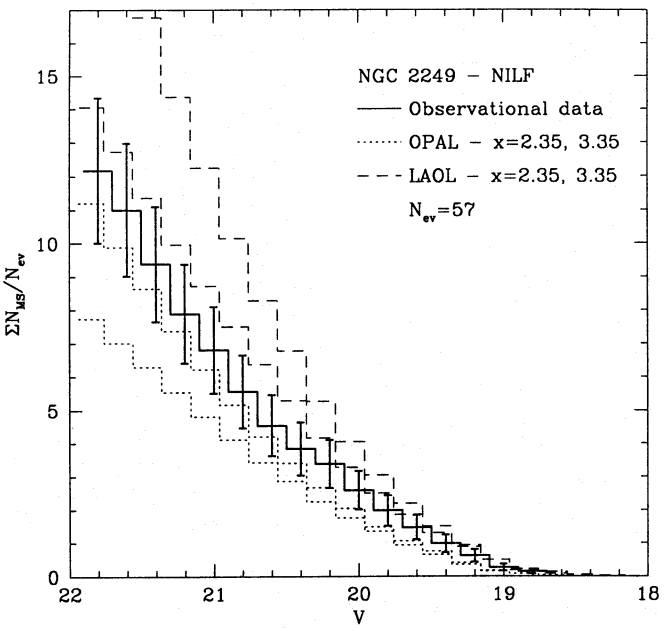


**Fig. 11b.** The same as in Fig. 11a but for NGC 2249. The theoretical NILFs are calculated assuming the age of 5.5 $\times 10^8$ yr. The color excess in use is $E_{B-V}$ = 0.25

**Table 3.** Lifetimes and lifetime ratios; overshoot

| | OPAL | | LAOL | | |
|---|---|---|---|---|---|
| $M/M_\odot$ | $\tau_H$ | $\tau_{He}/\tau_H$ | $\tau_H$ | $\tau_{He}/\tau_H$ | $(\tau_{He}/\tau_H)_{OPAL}/(\tau_{He}/\tau_H)_{LAOL}$ |
| 2.5 | 5.138E8 | 0.335 | 5.497E8 | 0.215 | 1.56 |
| 3.0 | 3.291E8 | 0.253 | 3.429E8 | 0.150 | 1.69 |
| 4.0 | 1.697E8 | 0.140 | 1.695E8 | 0.100 | 1.40 |
| 5.0 | 1.049E8 | 0.097 | 1.005E8 | 0.086 | 1.12 |
| 7.0 | 5.234E7 | 0.069 | 4.920E7 | 0.075 | 0.92 |
| 9.0 | 3.238E7 | 0.061 | 3.032E7 | 0.069 | 0.88 |

**Table 4.** Lifetimes and lifetime ratios; classical mixing

| | OPAL | | LAOL | | |
|---|---|---|---|---|---|
| $M/M_\odot$ | $\tau_H$ | $\tau_{He}/\tau_H$ | $\tau_H$ | $\tau_{He}/\tau_H$ | $(\tau_{He}/\tau_H)_{OPAL}/(\tau_{He}/\tau_H)_{LAOL}$ |
| 2.5 | 3.783E8 | 0.672 | 4.132E8 | 0.467 | 1.44 |
| 3.0 | 2.456E8 | 0.550 | 2.608E8 | 0.373 | 1.47 |
| 4.0 | 1.305E8 | 0.326 | 1.302E8 | 0.259 | 1.26 |
| 5.0 | 8.220E7 | 0.231 | 7.874E7 | 0.210 | 1.10 |
| 7.0 | 4.291E7 | 0.143 | 3.949E7 | 0.161 | 0.89 |
| 9.0 | 2.710E7 | 0.113 | 2.468E7 | 0.135 | 0.84 |

voke the occurrence of convective overshoot in order to reproduce the morphology of the CMDs and the slope of the NILFs of the Large Magellanic Cloud clusters. It goes without saying that in order to draw the above conclusion, homogeneous grids of stellar models must be used. The grids to our disposal possess the desired degree of homogeneity. Specifically, models are available that differ either in the mixing scheme or in the opacity.

The adoption of classical models alters the age assigned to the clusters. In the case of NGC 2134, classical models suggest the age of $1 \times 10^8$ yr, with the turnoff mass of 5.3 $M_\odot$, and $3 \times 10^8$ yr with the turnoff mass 2.7 $M_\odot$ for NGC 2249.

As shown in Tables 3 and 4, now the lifetime ratio is $\tau_{He}/\tau_H$=0.21, compared to the value of $\tau_{He}/\tau_H$=0.14 for models with overshoot. In other words, with the classical models, the ratio $\tau_{He}/\tau_H$ is about a factor of 1.5 larger than obtained with overshoot scheme. Accordingly, we expect that the corresponding theoretical NILFs from classical models and models with overshoot should stay in similar ratio. The comparison of the NILFS obtained from classical and overshoot models at fixed opacity (OPAL) with the observational counterpart is shown in Figs. 12a (NGC 2134) and 12b (NGC 2249). In the case of NGC 2134, we find that theory and observation are in close agreement either for overshoot models and $x$ = 2.35 or classical models and $x$ = 3.35, even though for this latter case theoretical NILF tends to overestimate the observational one going towards fainter magnitudes. Reasonably, other values of $x$ can be excluded. The situation is more evident in the case of NGC 2249, where classical models with $x$ = 3.35 simply do not

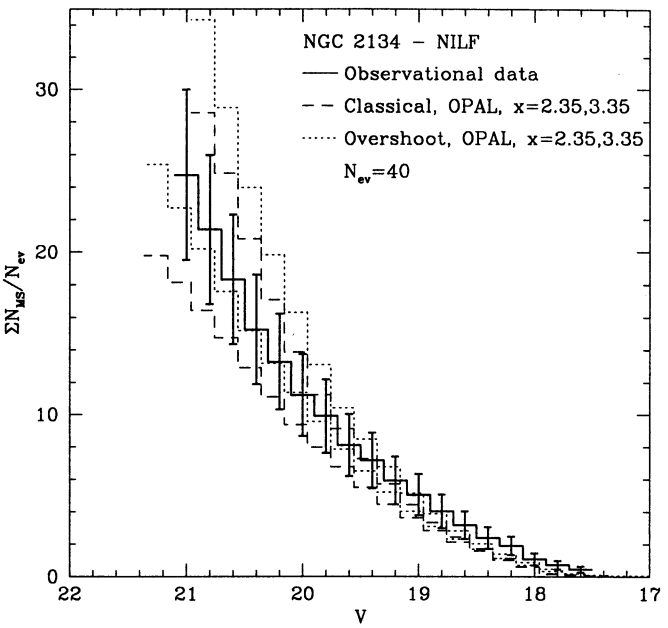


**Fig. 12a.** Comparison of the observational NILF for NGC 2134 with the theoretical ones obtained from classical (dashed lines) and overshoot (dotted lines) models. The theoretical NILFs are calculated with OPAL, a suitable fraction of binary stars, and different values of the IMF slope $x$ as indicated. The age is $1.9 \times 10^8$ yr for models with overshoot and $1 \times 10^8$ yr for classical models. For each group, the slope of the IMF gets steeper going upward. Absolute magnitudes are converted to apparent ones assuming $(m - M)_o$ = 18.5 and $E_{B-V}$ = 0.22

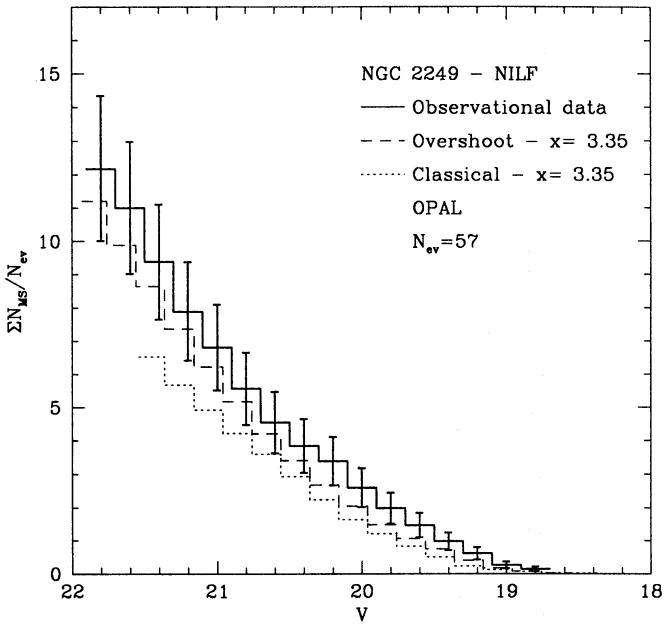


**Fig. 12b.** The same as in Fig. 12a but for NGC 2249. Now the age of models with convective overshoot is $5.5 \times 10^8$ yr and $3 \times 10^8$ yr for classical models. the color excess in use is $E_{B-V} = 0.25$

match the observational NILF, whereas overshoot models with $x = 3.35$ marginally agree with the data. It seems that much higher values of $x$ should be required which however seem to be unlikely.

The suggestion arises that a somewhat higher efficiency of convective overshoot would yield NILFS in good agreement with the data even for the classical Salpeter slope.

## 6. Summary and conclusions

We have presented the Johnson $BV$ photometry of the stellar content of two clusters of the LMC, namely NGC 2134 and NGC 2249, together with two companion fields. The CMDs and LFs of the clusters have been analyzed with the aid of homogeneous grids of stellar models differing either in the opacity (OPAL versus LAOL) or in the mixing scheme (classical versus overshoot). The goals of this study are the acquisition of the photometric data, determination of the age, clarification of the effects separately caused by the opacity and mixing scheme on the properties of the CMD and LF. The main results can be summarized as follows:

1. Adopting the distance modulus of $(m-M)_o = 18.5$mag, the overall morphology of the CMDs of both clusters is best matched by stellar models with metallicity Z=0.008 almost independently of the opacity in usage. Furthermore, the color excess of NGC 2134 is $E(B-V) \simeq 0.22$, while that of NGC 2249 is $E(B-V) \simeq 0.25$.

2. Adopting stellar models with convective overshoot and OPAL, the age of NGC 2134 turns out to be $1.9 \times 10^8$ yr, while the age of NGC 2249 is $5.5 \times 10^8$ yr. Conversely, using models with the classical scheme of mixing and the same opacity the age of NGC 2134 and NGC 2249 are decreased to $1 \times 10^8$ yr and $3 \times 10^8$ yr, respectively.

3. The above ages do not change significantly using the LAOL opacity for the simple reason that the core H-burning lifetime remains unchanged passing from OPAL to LAOL. It is worth recalling that the dominant difference between the two opacities, namely the bump at a few thousand degrees, is located too far out in the star to significantly affect the inner structure and hence the lifetime.

4. As expected, the main effect of the new opacity arises during the core He-burning phase, which is less luminous and hence of longer duration with the OPAL. Therefore, the net effect is that in the CMD the group of red giants that corresponds to the core He-burning stages is fainter, and relatively more numerous with respect to main sequence stars than with LAOL. The lower luminosity of the red giant better agrees not only with data of NGC 2134 and NGC 2249, but also with data of other similar clusters of LMC such as NGC 2164, NGC 1831, NGC 1866 where at given turnoff luminosity and hence age, the red evolved stars have been found to be less luminous than the theoretical expectations (Vallenari et al. 1991, 1992). In order to reconcile the magnitude of the turnoff with the magnitude of the evolved stars, the suggestion was advanced that a certain percentage of unresolved binary stars (either optical or physical) is present, which would brighten the turnoff and therefore reduce the magnitude difference with respect to the clump of red stars. The lack of a direct evidence of a significant population of binary objects, even though their presence cannot be excluded, always constituted a point of weakness of this way out. Other possible causes of the discrepancy have been examined at some extent by Vallenari et al. (1992) to whom we refer. None of these was found fully satisfactory. OPAL reduces the magnitude difference and therefore alleviates the disagreement, even if it does not rule out it completely. In this study also we have allowed for a certain percentage of binary stars, in the conviction that most of them are optical binaries due to the insufficient resolution of the algorithm used to detect and measure stars in crowded frames.

5. The core He-burning lifetimes is longer in models with OPAL. As a consequence, the ratio $\tau_{He}/\tau_H$ becomes 35% to 60% higher than in the corresponding models with LAOL. Looking at the lifetimes reported in Tables 3 and 4, it is evident that the effect of the mixing scheme always dominates over that of opacity. Therefore classical models with OPAL cannot recover the $\tau_{He}/\tau_H$ ratio of models with overshoot and LAOL. The conflict between observational star counts and theoretical lifetimes from classical models still remains unless either the observations are severely incomplete, which likely is not the case, or other parameters are at work. The analysis of the NILF indicates that, in order to fit the data, even with OPAL, classical models should require steeper slopes of the IMF, $x = 3.35$ or greater, while models with overshoot and OPAL are consistent with the standard slope $x = 2.35$. Although the slope of the IMF is uncertain and slopes steeper than the Salpeter one have often been suggested, values higher than 3.35 are difficult to justify. Therefore, models with convective overshoot seem to better agree with the observational data than classical models

and perhaps the suggestion arises for more efficient overshoot than adopted in our models.

## References


Alongi, M., Bertelli, G., Bressan, A., Chiosi, C., Fagotto, F., Greggio, L., Nasi, E. 1993, A&AS, 97, 851

Anders, E., & Grevesse, N. 1989, Geochim. Cosmochim. Acta, 53, 197

Blöcker, T., Schönberner, G. 1991, A&A 244, L43

Bressan, A., Bertelli, G., Chiosi, C.1981, A&A, 102, 25

Bressan, A., Fagotto, F., Bertelli, G., Chiosi, C. 1993, A&AS 100,647

Brocato E., Buonanno R., Castellani V., Walker A.R., 1990, ApJS 71, 25

Castellani V., Chieffi A., Straniero O., 1990, ApJS 74, 463

Chiosi, C., Bertelli, G., Bressan, A. 1992, ARA&A, 30, 305

Chiosi, C., Bertelli, G., Meylan, G., Ortolani, S. 1989, A&A, 219, 167

Cassatella, A., Barbero, J., Geyer, E. H. 1987, ApJS, 64, 83

Elson, R. A. W., 1986, PhD Thesis, Cambridge University

Fagotto F., Bressan A., Bertelli G., Chiosi C. 1993a, A&AS, submitted

Fagotto, F., Bressan, A., Bertelli, G., Chiosi, C. 1993b, A&AS submitted

Grevesse, N. 1991, A&A, 242, 488

Hannaford, P., Lowe, R. M., Grevesse, M., Noels, A. 1992, A&A, 259,301

Hanuschik, R. W., Schimidt-Kaler, T. 1991, A&A, 249, 36

Hodge, P. W., & Schommer, R. A. 1984, PASP, 96, 28

Huebner, W. F., Mertz, A. L., Magee, N. H., Argo, M. F. 1977, Los Alamos Scientific Laboratory Report, no. LA-6760-M

Iglesias, C. A., Rogers, F. J., Wilson, B. C. 1992, ApJ, 397, 717

Jones J.H., 1987, AJ 94, 347

Landolt, A.U., 1983, AJ 88, 439

Meynet G., Mermilliod J.C., Maeder A., 1993, A&AS 98, 477

Panagia, N., Gilmozzi, R., Macchetto, F., Adorf, H. M., Kirshner, R. P. 1991, ApJ, 380, L23

Rogers, F. J., Iglesias, C. A. 1992, ApJS, 79, 507

Schmidt-Kaler, Th. 1982, Landolt-Börnstein, Group VI, vol. 2b, pag. 1, Springer-Verlag, Berlin, Heidelberg, New York

Searle, L., Wilkinson, A., Bagnuolo, W. 1980, ApJ, 239, 803

Stetson, P. B. 1987, PASP, 99, 191

Stetson, P. B., Harris , W.E., 1988, AJ, 96, 909

Stothers, R.B., Chin C.W., 1991, ApJ 381, L67

Vallenari, A., Chiosi C., Bertelli G., Meylan G., Ortolani S., 1991, A&AS 87, 517

Vallenari, A., Chiosi C., Bertelli G., Meylan G., Ortolani S., 1992, AJ, 104, 1100

van den Berg, S., 1981, A&AS 46, 79

Westerlund, B. E. 1991, A&AR, 2, 29

Westerlund, B. E., Azzopardi, M., Breysacher, J., Rebeirot, E. 1991, A&AS 91, 425


This article was processed by the author using Springer-Verlag LaTeX A&A style file version 3.